

## Material Synthesis, Spectral, Optical and Antimicrobial Activity of Imidazolium Based Aldehydic Ionic Liquids: 1-Ethyl-3-methyl-2-(2-oxo-ethyl)-3H-imidazol-1-ium bromide (I) and 1-Butyl-3-methyl-2-(2-oxo-ethyl)-3H-imidazol-1-ium chloride (II)

J. Sudhalakshmi, K. Rajathi\*

PG & Research Department of Chemistry, Kalaingar Karunanidhi Government Arts College, Tiruvannamalai-606603, Affiliated to Thiruvalluvar University, Serkkadu, Vellore, Tamil Nadu, India

Received 26 December 2022, accepted in final revised form 14 June 2023

### Abstract

We successfully produced imidazolium aldehydes from imidazolium alcohols for the first time using copper wire and no oxidizing agents. The findings of IR, UV, <sup>1</sup>H-NMR, and <sup>13</sup>C-NMR spectral examinations all indicated complete oxidation of the alcohols, which was further demonstrated by those findings. The oxidation technique was used to create the ionic liquids 1-Ethyl-3-methyl-2-(2-oxo-ethyl)-3H-imidazol-1-ium; bromide and 1-Butyl-3-methyl-2-(2-oxo-ethyl)-3H-imidazol-1-ium; chloride. Using elemental and spectral analyses confirmed the structure of the synthesized compounds (I) and (II). FT-IR analysis was used to determine the presence of functional groups in the grown samples (I) and (II), and <sup>1</sup>H-NMR and <sup>13</sup>C-NMR spectral analysis were performed to confirm the environment of the elements (C, H). A UV-Visible-NIR spectrophotometer was implemented to determine the optical absorption value for samples (I) and (II). Using DSC analysis, the thermal stability and decomposition were seen. *Bacillus Cereus*, *Staphylococcus Aureus*, *Enterobacter Coacae*, and *Staphylococcus Haemolyticus* were used in an antimicrobial study for samples (I) and (II), and the results are compared with control Ciprofloxacin.

**Keywords:** Imidazolium ionic liquids; Fourier transform infrared spectroscopy (FT-IR); NMR; UV; TG-DTA analysis; Antimicrobial analysis.

© 2023 JSR Publications. ISSN: 2070-0237 (Print); 2070-0245 (Online). All rights reserved.  
doi: <http://doi.org/10.3329/jsr.v15i3.63522> J. Sci. Res. 15 (3), 793-806 (2023)

### 1. Introduction

Ionic liquids are crucial to the production of green solvents. The ionic liquid is used extensively in chemistry, biochemistry, and industrial (pharmaceutical) applications [1]. Salts known as ionic liquids have melting points under 100 °C and are made entirely of polar ions, including organic cations and inorganic anions [2]. Due to their high ionic density, fluidity, and little vapor pressure, ionic liquids have undergone substantial research. Due to the tenability and adaptability of ionic liquid behavior, ILs have been

---

\*Corresponding author: [rajathi\\_sridhar@rediffmail.com](mailto:rajathi_sridhar@rediffmail.com)

exploited for a variety of applications in academia and industry [1,3]. Due to their low vapor pressure and non-toxic ions, ILs are often safer solvents [4].

Environmentally acceptable solvents for enzymatic and chemical procedures include ionic liquids based on imidazolium, pyridinium, and quaternary ammonium cations [5]. In the methanolysis of  $\text{NaBH}_4$ , synthesized and characterized polymeric ionic liquid microgels based on imidazolium showed excellent catalytic activity [6]. Ionic solutions with an imidazolium base have recently been employed as inhibitors to stop metal corrosion in acidic environments [7]. The alkyl chain length and size of imidazole-based ionic liquids affect how active they are. It is frequently employed in industrial processes like acid pickling and acid descaling [8,9]. Due to the intrinsic magnetic, spectroscopic, and electrochemical characteristics of ionic liquids that depend on the confined metal ions, synthesized and characterized metals containing ionic liquids have high electro-catalytic activity [10,11]. The zinc (II) combination with imidazolium ionic liquid tag demonstrated effective DNA breakage and antifungal and antibacterial activity against gram-positive bacteria [4,11,12].

Because of the great electrochemical stability in oxidation that synthetic fluorinated imidazolium ILs shows, it may be employed as an electrolyte for lithium-ion batteries [5, 13]. Ionic liquids with imidazolium bases are employed as efficient liquid media for the creation of nanoparticles and can serve as stabilizers of nanoparticles at room temperature [14,15].

Due to its simple tunable, designer, non-toxic, non-flammable, and low volatility qualities, imidazolium-based ILs are usually considered a green solvent since they may be utilized for synthesis, catalysis, solar cell, and desulfurization of fuel applications in a variety of disciplines [16]. 1,2-azido alcohols were created utilizing a magnetic catalyst and dicationic ionic liquid at room temperature. Short reaction times, high yields, ease of purification, and reusable catalysts are some benefits of ionic liquids as good catalytic activity [8,17]. Scientists in this sector recommended Ionic liquids as greener alternatives to conventional organic solvents because of their superior physicochemical characteristics [18-21].

There is no announcement planned about the use of 'Cu' wire in the manufacture of aldehydes from alcohol. As a result, we decided to create 1-Ethyl-3-methyl-2-(2-oxo-ethyl)-1-butyl-3-methyl-2-(2-oxo-ethyl) and -3H-imidazol-1-ium bromide (I) without using reducing agents, -3H-imidazol-1-ium chloride (II) aldehydic compounds from their corresponding alcohols.

## **2. Experimental Procedure**

### **2.1. Chemicals**

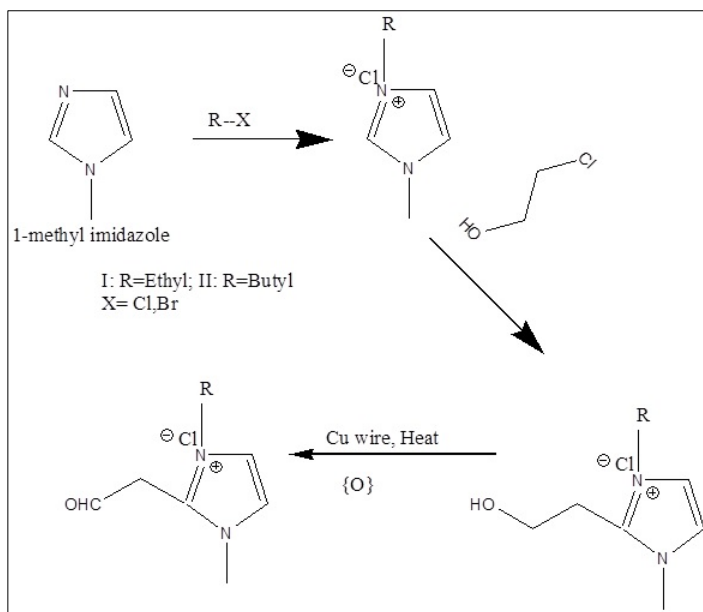
Sigma Aldrich, Merk, and SD Fine Chemical Limited provided AR grade 1-methyl imidazole, chloroethanol, sodium hydride, acetonitrile, bromoethane, and chlorobutane, which were kept and utilized without additional purification. On TLC plates, the product

homogeneity was examined. In addition, the oxidation process employed the copper wire that was acquired.

## 2.2. Synthesis of ionic liquids

**Synthesis of 1-Ethyl-3-Methyl- 3H-imidazol-1-ium bromide:** The round bottom flask was filled with an equimolar mixture of 1-methylimidazole [MIM] (24.63 g, 0.3 mol) and bromoethane (32.69 g, 0.3 mol). The resultant viscous liquid formation was cooled to room temperature and dried under vacuum after being vigorously agitated and refluxed at 70 °C for 48 h in a nitrogen environment (16.5 g, Yield 87 %).

**Synthesis of 1-Ethyl-2-(2-hydroxy-ethyl)-3-methyl-3H-imidazol-1-ium bromide:** A stirred solution of the previously produced 1-ethyl-3H-imidazole-1-ium bromide (19.0 g, 0.1mol) in acetonitrile (50 mL) was given NaH (3.6 g, 0.15 mol). After the reaction mixture had been agitated for 4 h, the chloroethanol (8.05 g, 0.1 mol) was added, and the process was then repeated for another 24 h. Before the solution was evaporated to dryness and rinsed with ether (3×20 mL) to remove any excess alkyl halide, the reaction mixture's byproduct NaCl was filtered out. The remaining volatiles were removed under vacuum (19 g, Yield 82 %).



Scheme 1. Synthetic route of sample I: 1-Ethyl-3-methyl-2-(2-oxo-ethyl)-3H-imidazol-1-ium bromide; sample II: 1-Butyl-3-methyl-2-(2-oxo-ethyl)-3H-imidazol-1-ium chloride

**Synthesis of 1-Ethyl-3-methyl-2-(2-oxo-ethyl)-3H-imidazol-1-ium bromide:** Semi micro boiling tube was filled with 1-Ethyl-3-methyl-2-(2-oxo-ethyl)-3H-imidazol-1-ium bromide. Then a heated copper spiral wire was inserted into this little tube. Ten to fifteen times, the exact identical process was performed. Regular chemical tests were used to validate and confirm the production of the aldehyde product. Here, dehydrogenation takes place while warmed copper (573 K) is submerged in an alcohol solution, which causes the creation of the corresponding aldehydes (Yield 74 %). No filtering methods were necessary for this oxidation technique. All three methods mentioned above were employed to create 1-Butyl-3-methyl-2-(2-oxo-ethyl)-3H-imidazol-1-ium chloride.

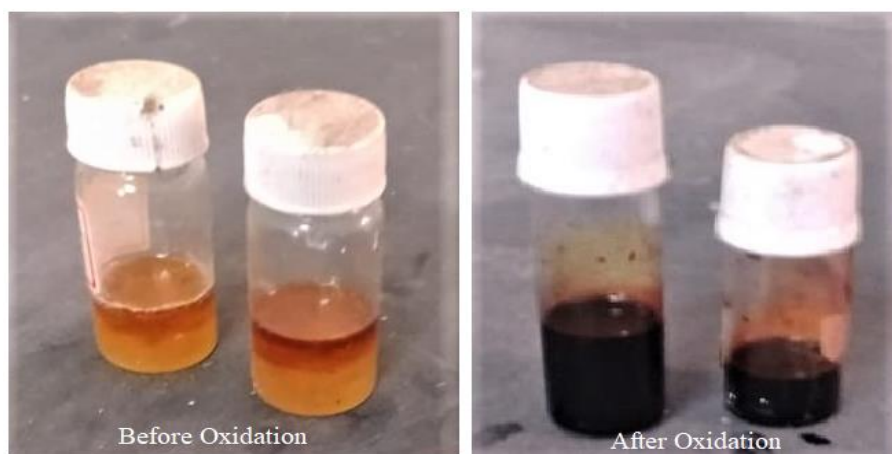


Fig. 1. Before and after oxidation of sample I: 1-Ethyl-3-methyl-2-(2-oxo-ethyl)-3H-imidazol-1-ium bromide; sample II: 1-Butyl-3-methyl-2-(2-oxo-ethyl)-3H-imidazol-1-ium chloride.

### 2.3. Characterization techniques

The purity of ILs was checked by  $^1\text{H}$  NMR spectroscopy. NMR spectra were recorded on 400 MHz Varian spectrometer at ambient probe temperature and referenced to internal TMS. The FTIR analysis was performed in a Bruker Alpha-P spectrometer (64 scans,  $4\text{cm}^{-1}$  of resolution). Thermogravimetric analysis (TGA) was performed in Q50 TA TGA operating under an oxidant atmosphere (flux of 100 mL/min). The samples (10-15 mg) were heated until 800 °C with a rate of  $20\text{ °C min}^{-1}$ . The diffuse reflectance spectra of all the catalysts were recorded in Shimadzu UV 2450 model equipped with an integrating sphere and using powdered  $\text{BaSO}_4$  as a reference. A pathogenic bacterial strain was used to evaluate the antibacterial capabilities. A good diffusion assay was performed to evaluate the antibacterial activity of samples I and II using gram-positive *Bacillus cereus* and gram-negative *Staphylococcus aureus*.

### 3. Results and Discussion

#### 3.1. Fourier transform infrared spectroscopy analysis

The modifications and existence of the functional group in the synthesized molecule were identified using FT-IR. FT-IR was performed using a Fourier Transform Infrared spectrophotometer in the 400 to 4000  $\text{cm}^{-1}$  range. We may deduce from the absorption values that the absorption band in the IR spectra (Fig. 2) represented the change in carbon number in samples I and II. Table 1 depicts this shift in absorption.

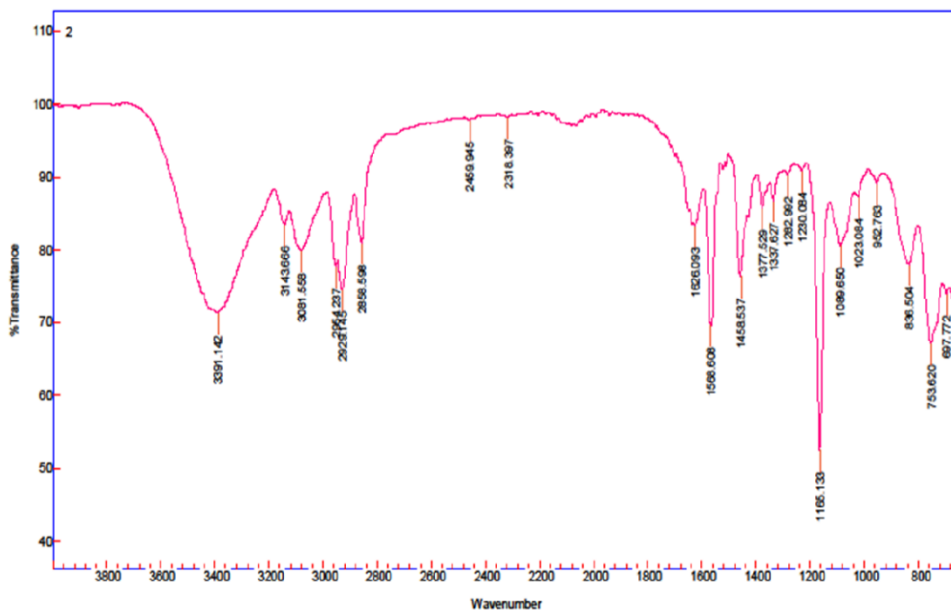


Fig. 2. a) FT-IR spectrum of 1-Ethyl-3-methyl-2-(2-oxo-ethyl)-3H-imidazol-1-ium bromide (I).

Table 1. Comparative wave band assignments of 1-Ethyl-3-methyl-2-(2-oxo-ethyl)-3H-imidazol-1-ium bromide (I) and 1-Butyl-3-methyl-2-(2-oxo-ethyl)-3H-imidazol-1-ium chloride (II)

Frequencies of absorption bands wavenumber ( $\text{cm}^{-1}$ )		Peak Assignments
Sample I	Sample II	
3391,3143,3081	3356	C-H stretching vibration of aromatic ring
2954,2929	2954	C-H stretching vibration of aldehyde
2858	2873	C-H stretching vibration of alkyl chain
1626	1633	C=O stretching vibration of aldehyde
1568	1571	C=N stretching vibration
1458	1489	C=C stretching vibration
1337	1386	C-N stretching vibration

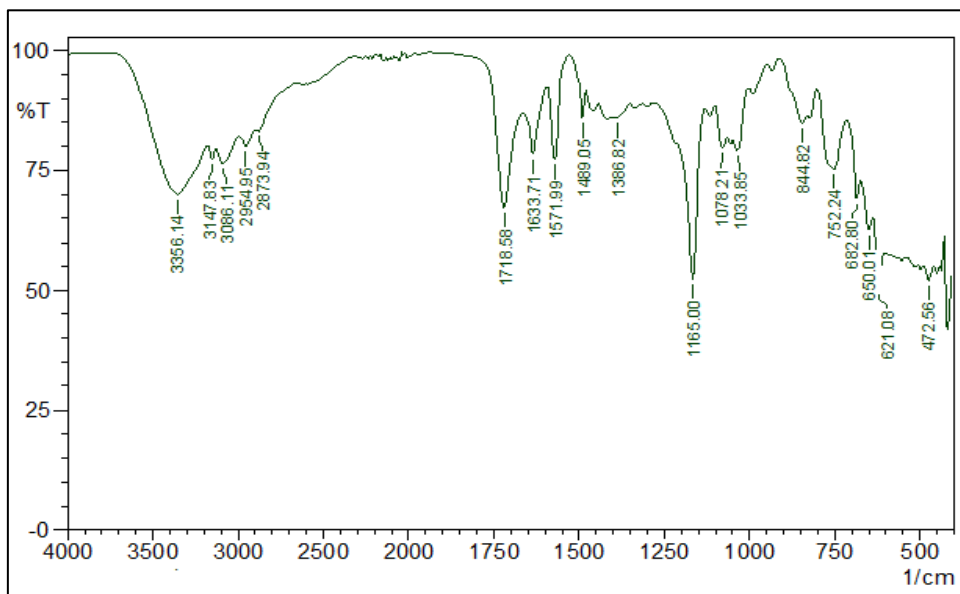


Fig. 2. b) FT-IR spectrum of 1-Butyl-3-methyl-2-(2-oxo-ethyl)-3H-imidazol-1-ium chloride (II).

**3.2. UV-Visible-NIR spectrophotometer analysis**

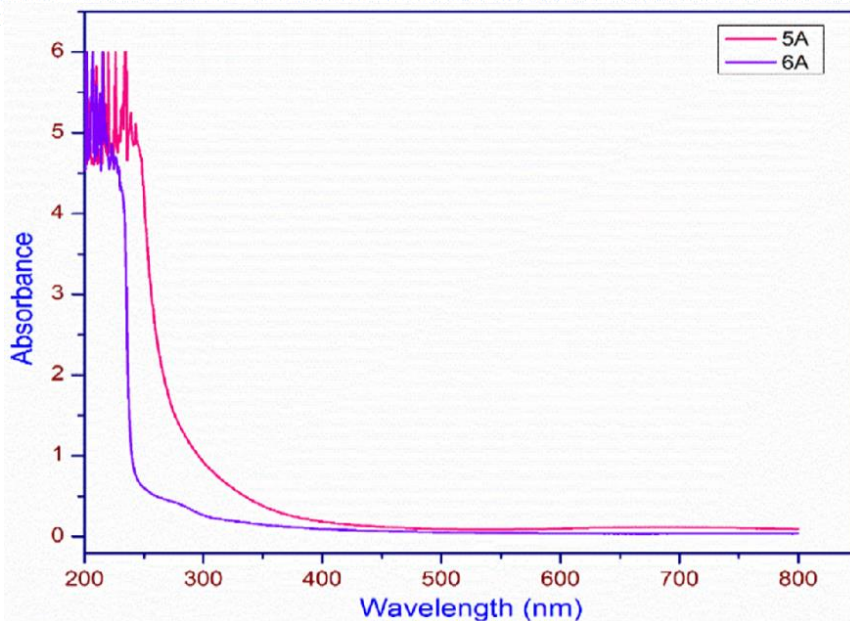


Fig. 3. Optical absorption spectrum of 1-Ethyl-3-methyl-2-(2-oxo-ethyl)-3H-imidazol-1-ium bromide (I) and 1-Butyl-3-methyl-2-(2-oxo-ethyl)-3H-imidazol-1-ium chloride (II).

### 3.3. $^1\text{H-NMR}$ and $^{13}\text{C-NMR}$ spectral analysis

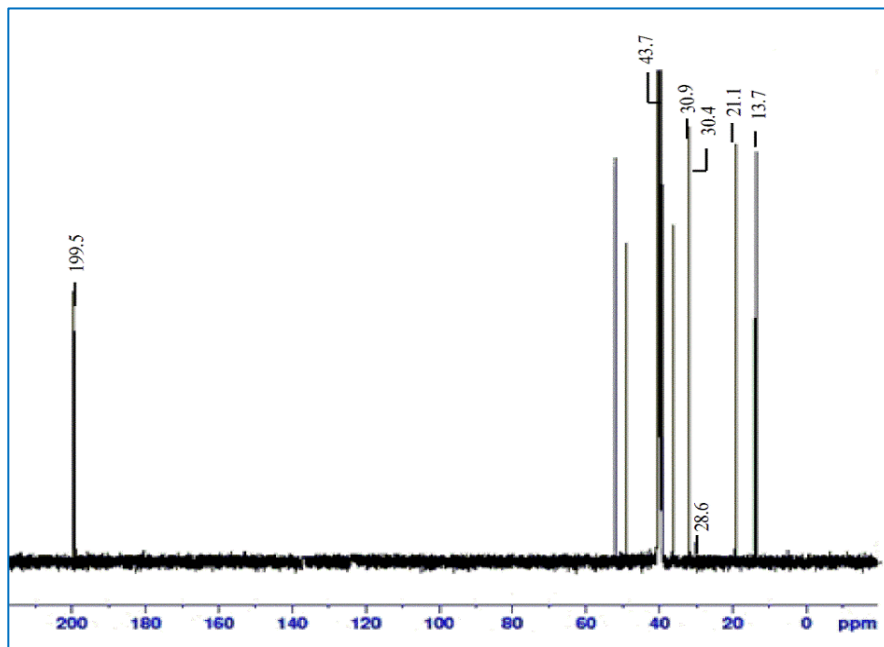


Fig. 4a.  $^{13}\text{C}$  NMR spectrum of 1-Ethyl-3-methyl-2-(2-oxo-ethyl)-3H-imidazol-1-ium bromide (I).

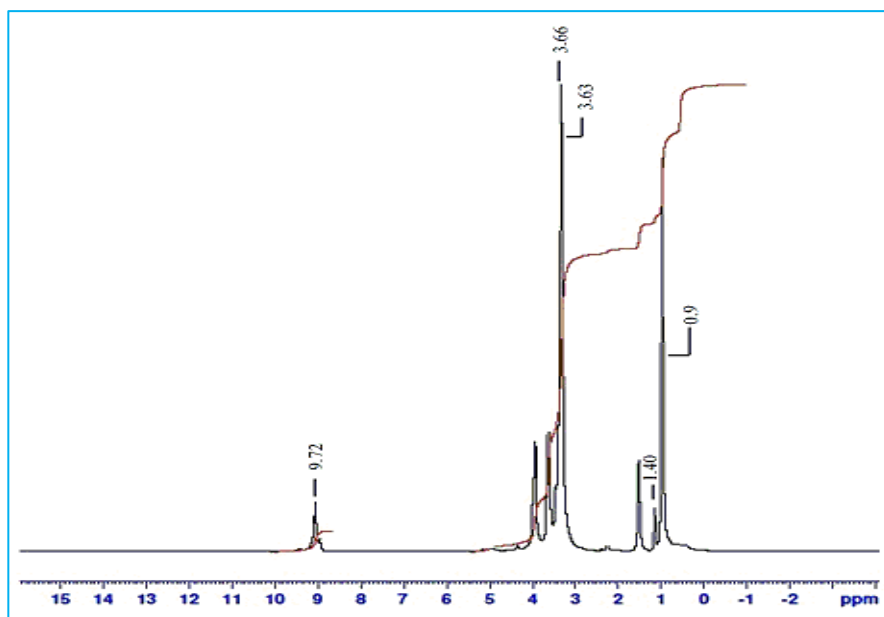


Fig. 4b.  $^1\text{H}$  NMR spectrum of 1-Ethyl-3-methyl-2-(2-oxo-ethyl)-3H-imidazol-1-ium bromide (I).

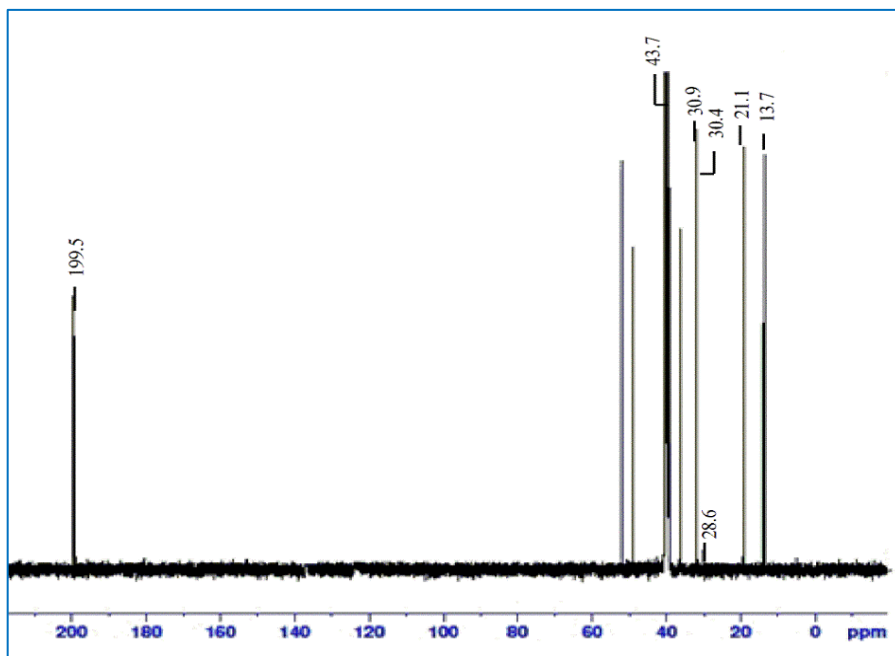


Fig. 5a.  $^{13}\text{C}$  NMR spectrum of 1-Butyl-3-methyl-2-(2-oxo-ethyl)-3H-imidazol-1-ium chloride (II).

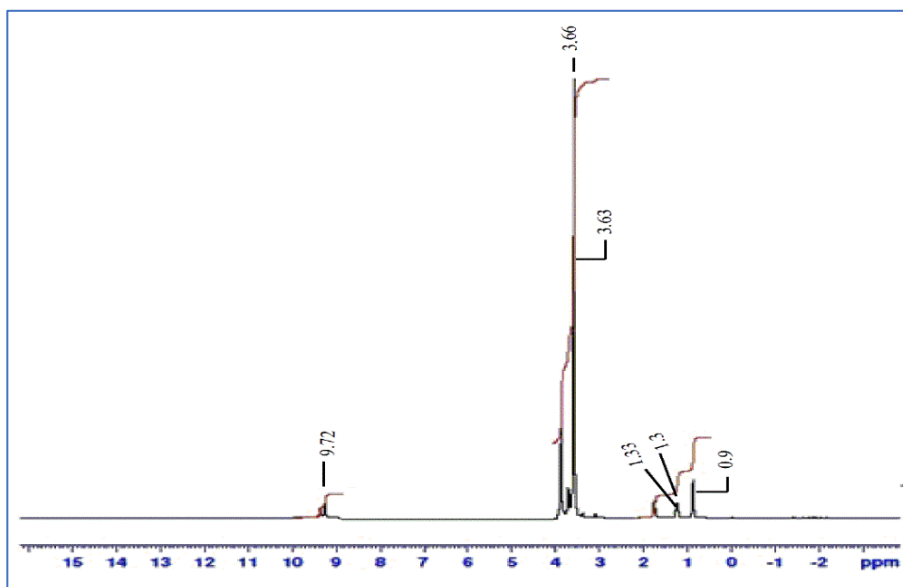


Fig. 5b.  $^1\text{H}$ -NMR spectrum of 1-Butyl-3-methyl-2-(2-oxo-ethyl)-3H-imidazol-1-ium chloride (II).

1-Ethyl-3-methyl-2-(2-oxo-ethyl)-3H-imidazol-1-ium bromide (I) and 1-Butyl-3-methyl-2-(2-oxo-ethyl)-3H-imidazol-1-ium chloride (II) were synthesized and submitted to  $^1\text{H}$  and  $^{13}\text{C}$ -NMR spectral analysis for structural clarity, as shown in Figs. 4 (a, b) and 5(a, b). At a doublet peak (3.66 ppm), influences of the NH group on proton from both sides were found. The signal in the  $^1\text{H}$ -NMR spectrum of about -9.8 ppm in both samples suggests that the aldehyde was formed via oxidation from the alcohol. Figs. 4 and 5 also illustrate the observed values.  $^{13}\text{C}$  NMR:  $\delta$  199.5, 36.8, 30.9, 30.4, 10.1 and  $^1\text{H}$  NMR:  $\delta$  9.72 (t, 1H), 3.66 (d, 2H), 3.63 (s, 3H), 1.40(q, 2H), 0.9 (t, 3H) for 1-Ethyl-3-methyl-2-(2-oxo-ethyl)-3H-imidazol-1-ium bromide (I).  $^{13}\text{C}$  NMR:  $\delta$  199.5, 43.7, 30.9, 30.4, 28.6, 21.1, 13.7 and  $^1\text{H}$  NMR:  $\delta$  9.72(t, 1H), 3.66(d, 2H), 3.63(s, 3H), 1.33(m, 2H), 1.3(m, 2H), 0.09 (t, 3H) for 1-Butyl-3-methyl-2-(2-oxo-ethyl)-3H-imidazol-1-ium chloride (II).

### **3.4. Differential scanning calorimeter (DSC) analysis**

The study employed DSC analysis (TG-DTA) on a NETZSCH SDA 449F with an  $\text{N}_2$  environment between 25 and 400  $^\circ\text{C}/\text{min}$ . Fig. 6 displays the DSC-TGA curves of sample (I) and sample (II). Data on thermal degradation of the total percent mass loss in ionic liquids (IL) made from imidazolium were collected using TGA. The findings are represented visually and highlight compounds I and II's thermal stability. Due to the hydrophilic nature of imidazolium ionic liquids at temperatures below 200  $^\circ\text{C}$ , a small weight loss occurs below 100  $^\circ\text{C}$  due to residual organic solvent and water being physically observed. As a result, weight loss occurred for samples at temperatures ranging from room temperature to 232  $^\circ\text{C}$ , which was attributed to the degradation of organic remains. [20,21]. It is clear that Sample I has the highest thermal stability above 325  $^\circ\text{C}$ , proving that stability rises with the length of the cationic alkyl chain. Compound I goes through a two-state breakdown when heated in an inert environment, although this has not happened yet. When Compound II is heated in an inert environment, a two-state breakdown occurs. Around 25  $^\circ\text{C}$  to 225  $^\circ\text{C}$  is the first decomposition temperature range. This results from the removal of moisture that was present in the joints. At 225  $^\circ\text{C}$ , the second breakdown begins without the presence of ionic liquids.

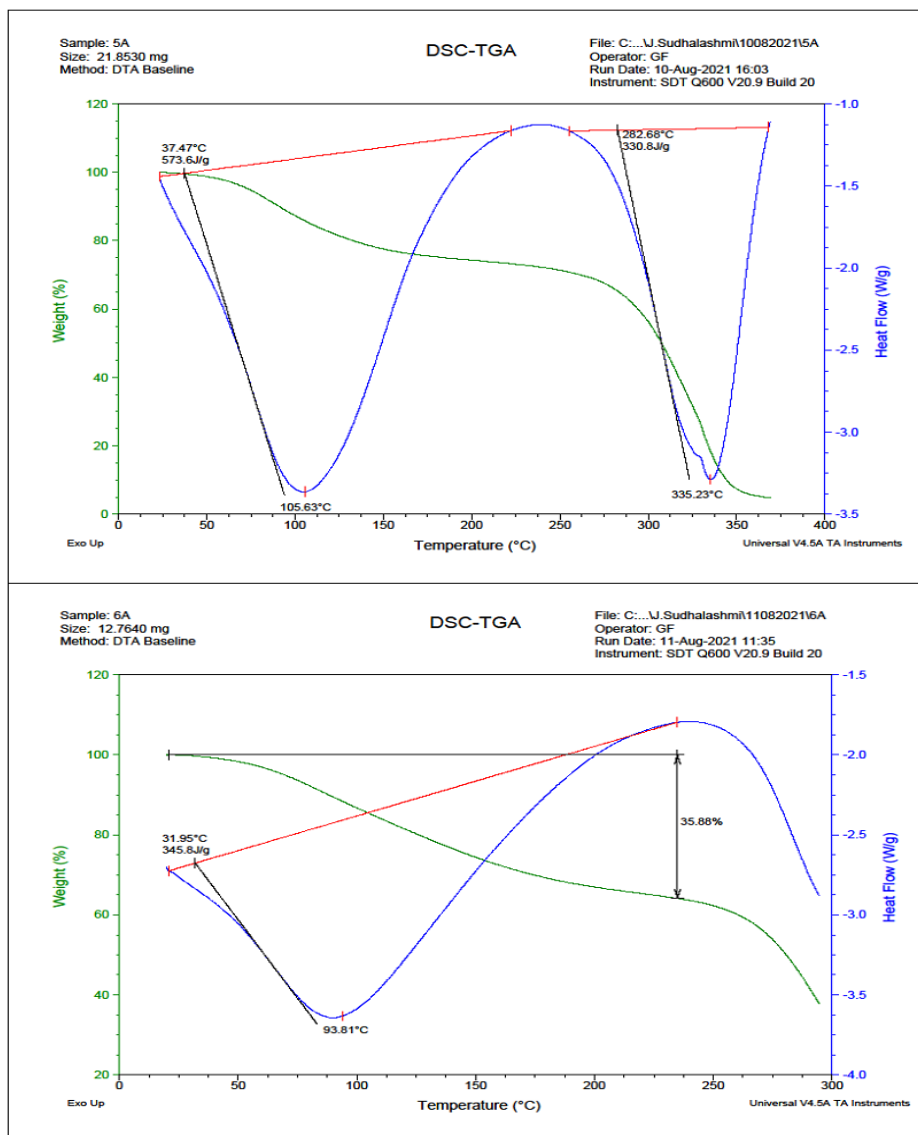


Fig. 6. DSC-TGA analysis of 1-Ethyl-3-methyl-2-(2-oxo-ethyl)-3H-imidazol-1-ium bromide (I) and 1-Butyl-3-methyl-2-(2-oxo-ethyl)-3H-imidazol-1-ium chloride (II).

### 3.5. Antimicrobial activity

To find out the antibacterial activity of 1-Ethyl-3-methyl-2-(2-oxo-3 ethyl)-3H-imidazol-1-ium bromide (I) and 1-Butyl-3-methyl-2-(2-oxo-ethyl)-4 3H-imidazol-1-ium chloride (II), three gram positive bacterias like *Bacillus Cereus*, *Staphylococcus Aureus* and *Staphylococcus Haemolytics* and one gram positive bacteria like *Enterobacter Cloacae* were used. And their zone of inhibition levels were displayed in Figs. 7 and 8. Bar

diagram 9, shows the antibacterial activity of sample I and II at various concentrations. The well diffusion assay was performed to evaluate the antibacterial activity of samples I and II. Muller Fresh bacterial cultures were dispersed over a sheet of Hinton agar that had been produced in 50 L quantities. The plates were incubated for 24 h at 37 °C, and the inhibitory zone's millimeter-sized size was measured. The antimicrobial test findings show that sample I is more active than sample II. The effects of the four distinct bacterial species were identical. The substituents at position 1 on the imidazole ring determine the efficiency of samples against bacterias.

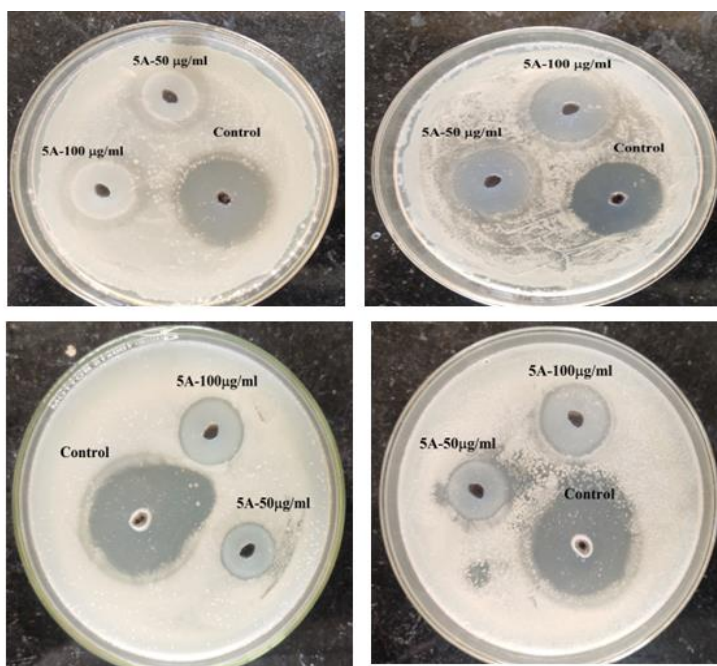


Fig. 7. Antimicrobial activity of 1–Ethyl-3-methyl-2-(2-oxo-ethyl)-3H-imidazol-1-ium bromide (I).

Table 2. Comparative Antimicrobial values of 1–Ethyl-3-methyl-2-(2-oxo-ethyl)-3H-imidazol-1-ium bromide (I) and 1-Butyl-3-methyl-2-(2-oxo-ethyl)-3H-imidazol-1-ium chloride (II).

Sample	Concentration (µg/mL)	<i>Enterobacter Cloacae</i> (Gram Negative)	<i>Staphylococcus Haemolyticus</i> (Gram Negative)	<i>Bacillus Cereus</i> (Gram Positive)	<i>Staphylococcus Aureus</i> (Gram Positive)
I	100µg/mL	10	12	10	11
	50µg/mL	9	10	8	9
	Control (Ciprofloxacin)	15	16	17	17
II	100µg/mL	10	10	10	10
	50µg/mL	9	9	8	9
	Control (Ciprofloxacin)	17	16	17	17

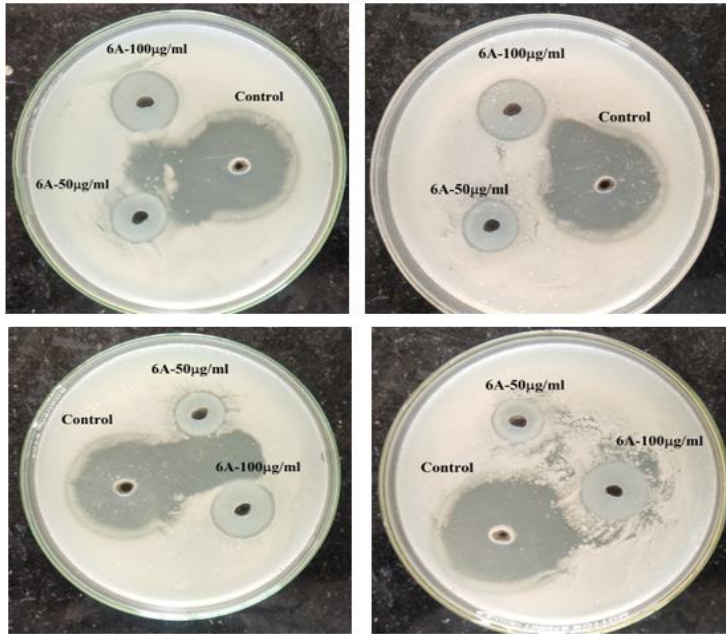


Fig. 8. Antimicrobial activity of 1-Butyl-3-methyl-2-(2-oxo-ethyl)-3H-imidazol-1-ium chloride (II).

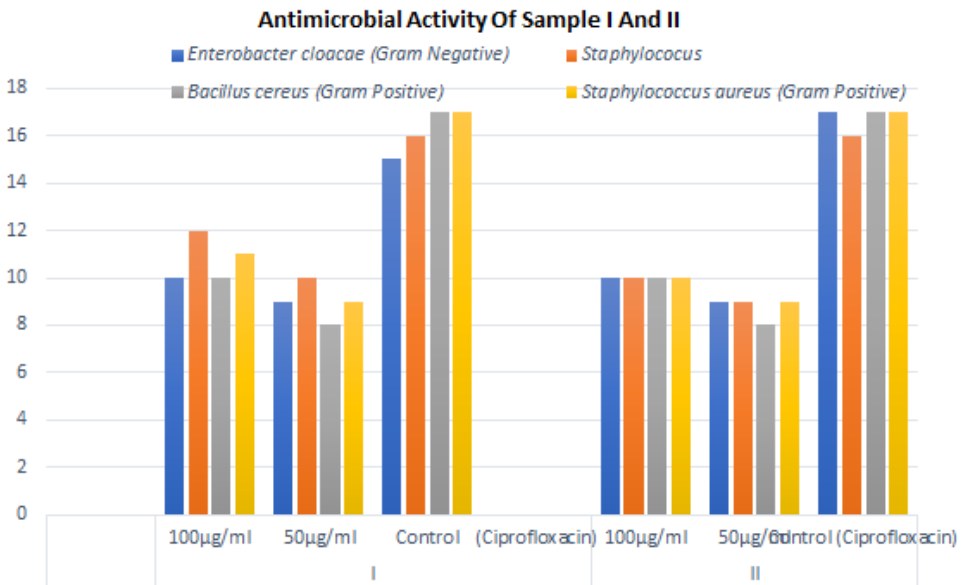


Fig. 9. Comparative Antimicrobial activity bar diagram of 1-Ethyl-3-methyl-2-(2-oxo-ethyl)-3H-imidazol-1-ium bromide (I) and 1-Butyl-3-methyl-2-(2-oxo-ethyl)-3H-imidazol-1-ium chloride (II).

#### 4. Conclusion

The chemicals 1-Butyl-3-methyl-2-(2-oxo-ethyl)-3H-imidazol-1-ium chloride (II) and 1-Ethyl-3-methyl-2-(2-oxo-ethyl)-3H-imidazol-1-ium bromide (I) were produced using the oxidation technique. In this procedure, turning alcohol into aldehydes, 'Cu' wire worked well. The FT-IR spectrum analysis of samples I and II showed that the synthesis of the carbonyl group exhibits peaks of about 1700  $\text{cm}^{-1}$ . According to the UV-Visible-NIR spectrum, the optical absorption for both samples with lower absorbance was found at 290 nm. Spectral analysis using the  $^1\text{H}$  and  $^{13}\text{C}$ -NMR further validated the aldehyde's synthesis. The compounds I and II are thermally stable but exhibit two-state breakdowns when heated in an inert environment, according to the TG-DTA study. When the observed values from an antimicrobial study using gram-positive bacteria *Bacillus Cereus*, *Staphylococcus Aureus*, and gram-negative bacteria *Enterobacter Cloacae*, *Staphylococcus Haemolytics* were compared with the control antibiotic *Ciprofloxacin*, it was found that compounds I and II had lower efficacy. It is evident from the exceptional optical and thermal stability of synthetic compounds I and II that they are used in a range of biological processes.

#### References

1. K. Matsumoto, T. Yano, S. Date, Y. Odahara, and S. Narimura, Polym. Bull. **11**, 6 (2020). <https://doi.org/10.1007/s00289-020-03364-4>
2. L Song, R. Wang, K. Niu, Y Liu, et al., Colloids Surf. A **609**, ID 125666 (2021). <https://doi.org/10.1016/j.colsurfa.2020.125666>
3. T. Misawa, J. Kobayashi, Y. Kiyota, M. Watanabe, et al., Materials **12**, ID 2283(2019). <https://doi.org/10.3390/ma12142283>
4. B. Sinha and S. Saha, Intech Open 1 (2019). <https://doi.org/10.5772/intechopen.86379>
5. K. Chatterjee, A. D. Pathak, A. Lakma, C. S. Sharma, et al., Sci. Reports **10**, 9606 (2020). <https://doi.org/10.1038/s41598-020-66341-x>
6. A. Bordet, G. Moos, C. Welsh, P. Licence et al., ACS Catal. **10**, 13904 (2020). <https://doi.org/10.1021/acscatal.0c03559>
7. K. Bryant, E. Hammond-Pereira, and S. R. Saunders, J. Phys. Chem. B **125**, 253 (2021). <https://doi.org/10.1021/acs.jpcc.0c08908>
8. Z. Hormozinezhad, M. Gorjizadeh, N. Taheri, and S. Sayyahi, Bull. Chem. Soc. Ethiop. **32**, 309 (2018). <https://doi.org/10.4314/bcse.v32i2.10>
9. O. Naderi, M. Nyman, M. Amiri, and R. Sadeghi, J. Mol. Liq. **273**, 645 (2019). <https://doi.org/10.1016/j.molliq.2018.10.046>
10. M. E. EL-Hefnawy, A. M. Atta, M. El-Newehy, and A. I. Ismail, J. Mat. Res. Technol. **9**, 14682 (2020). <https://doi.org/10.1016/j.jmrt.2020.10.038>
11. D. M. Rodrigues, L. M. dos Santos, F. L. Bernard, I. S. Pinto, et al., SN Appl. Sci. **2**, 1936 (2020). <https://doi.org/10.1007/s42452-020-03712-z>
12. A. Dzienia, M. Tarnacka, K. Koperwas, P. Maksym, et al., Macromol. **53**, 6341 (2020). <https://doi.org/10.1021/acs.macromol.0c00783>
13. A. M. Curreri, S. Mitragotri, and E. E. L. Tanner, Adv. Sci. **8**, ID 2004819 (2021). <https://doi.org/10.1002/advs.202004819>
14. N. Wang, X. Zhou, and B. Cui, J. Chrom. A **1606**, ID 460376 (2019). <https://doi.org/10.1016/j.chroma.2019.460376>
15. W. N. Lee, N. M. Salleh, and S.-F. Cheng, Industr. Crops Prod. **170**, ID 113808 (2021). <https://doi.org/10.1016/j.indcrop.2021.113808>

16. L. I. Teodoro, S. A. Bellia, M. Zeller, P. C. Hillesheim, *Chem. Data Collect.* **35**, ID 100760 (2021). <https://doi.org/10.1016/j.cdc.2021.100760>
17. R. A. A. Talip, W. Z. N. Yahya, and M. A. Bustam, *Sustainability* **12**, 7598 (2020). <https://doi.org/10.3390/su12187598>
18. F. Ahmed, M. M. Rahman, S. C. Sutradhar, and N. S. Lopa, et al., *Electrochim. Acta* **302**, 161 (2019). <https://doi.org/10.1016/j.electacta.2019.02.040>
19. T. A. Bauer, J. Imschweiler, C. Muhl, B. Weber, and M. Barz, *Biomacromol.* **22**, 2171 (2021). <https://doi.org/10.1021/acs.biomac.1c00253>
20. H. N. Abdelhamid, *Int. J. Hydrogen Energy* **46**, 726 (2021). <https://doi.org/10.1016/j.ijhydene.2020.09.186>
21. N. Subasree and J. A. Selvi, *Heliyon* **6**, ID e03498 (2020). <https://doi.org/10.1016/j.heliyon.2020.e03498>